POAC'25
St. John's, Newfoundland and Labrador, Canada

Proceedings of the 28th International Conference on Port and Ocean Engineering under Arctic Conditions
Jul 13-17, 2025
St. John's, Newfoundland and Labrador
Canada

Comparative Analysis of Compressive Failure Mechanics of Ice due to Ice-Particle and Spherical Steel Indentation Tests

Thomas Fitzpatrick[1], Rocky S. Taylor[1], Jan Thijssen[2]
[1] Faculty of Engineering and Applied Science, Memorial University of Newfoundland, St. John's, NL Canada
[2] C-CORE, St. John's, NL Canada

ABSTRACT

The indentation of rock particles into ice is an important aspect of understanding subsea interactions involving ice features and gravelly soil. Much of the literature surrounding the compressive failure of ice due to indentation, and the associated indentation tests implemented to investigate this, are based on spherical steel indentation experiments. In an effort to investigate these types of indentations with conditions more closely approximate to gravelly soil on the ocean floor, this paper investigates the indentation of unconstrained rock particles into an ice specimen, where observations are made to study the effect of changes in rate on indentation. Experiments were conducted using samples of rocks ranging in size from 9.5mm-19.1mm with tests completed for an indentation depth of 7 mm at three indentation rates: 10 mm/s, 0.5 mm/s, and 0.01 mm/s. Maximum observed forces and pressures exerted onto the ice by the rock particles are examined and compared based on changes in the noted test parameters. These outcomes from the ice-rock tests were compared directly with outcomes from similar experiments completed with spherical steel indenters, reported from previously completed research programs. This comparison of experimental results shows good general agreement across the studied indentation rates. It highlights an analogous relationship between ice failure mechanics under compression for both spherical steel indenters and unconstrained rock particles under indentation conditions.

KEY WORDS: Ice Mechanics; Ice-Particle Indentation; Compressive Ice Failure; Spherical Steel Indenter; Rate Effects.

INTRODUCTION

To better understand natural processes associated with interactions between ice features and the ocean floor, a series of experiments have been conducted. These interactions are described by a phenomenon known as scouring, when scouring occurs, the soil on the ocean floor will push up against the ice feature and cause an accumulation of soil and gravel particles around the contact interface. These soil particles have the potential to embed and subsequently freeze themselves into the surface of the ice feature. These embedded particles would then serve to potentially act as "hard points" when placed under pressure in the event of contact with an engineered structure. These "hard points" would then transmit local pressures, having the potential to cause the embedded particles to act as stress concentrators that would weaken the ice and reduce peak local ice pressures. Alternatively, these could result instead in the creation of an "armored" ice layer which could increase local pressures transmitted through the ice. Therefore, the experimental tests presented herein study the initial phase of ice particle embedment through compressive ice indentation tests on test populations of single and multiple rock particles. The results of these tests are subsequently compared to those completed with spherical steel intenders to assess the similarities of ice under compressive indentation conditions.

Compressive loading of ice often results in complex mechanics of ice failure and resulting deformation processes which can produce intense local and global loads that dominate design in the case of interaction with offshore structures (ISO 19906, 2019). These deformations are strongly dominated by viscoelastic processes for low strain rates, while more prominent effects of fracture, damage, and microstructural change are observed as the strain rate is increased (Schulson and Duval, 2009). Overall ice behavior is strongly dependent on loading rates. High pressure zones (hpzs) are small zones of localized high pressure which are observed when ice fails due to compressive loading (Jordaan, 2001). These hpz are formed due to contact localization as the ice begins to spall and split, acting as features through which the majority of ice loads are transmitted (Jordaan, 2001). Specific mechanisms associated with spalling and crushing include dynamic recrystallization, microfracture, macrofracture, and localized pressure melting have been observed to cause significant influence on the overall formation and development of high-pressure zones (ISO 19906, 2019) (Jordaan, 2001) (Taylor and Richard, 2014). It has been observed that only 10% of the global interaction area is affected by hpzs (Taylor and Richard, 2014).

Experimental ice indentation and crushing testing have been completed both in the field and in laboratories in order to investigate the various mechanisms of ice failure and development of high-pressure zones which take place during the compressive failure of ice. These tests were developed to study the behavior and evolution of high-pressure zones at the ice-surface interface under different conditions, which included varying experimental parameters including temperature, indenter size, and indentation rate. Several series of experiments were completed by Jordaan (2001), Barrette et al. (2002), and Wells et al. (2010) using a Materials Testing System (MTS) inside a cold room facility, these tests were scaled experiments based on large scale field tests (Jordaan, 2001). A series of experiments completed by Barrette et al. (2002) investigated the effects of temperature and displacement rate on the development of high-pressure zones. These experiments were completed within a code room facility and utilized a Materials Testing System (MTS) test frame. For these experiments an indentation depth of 2.6 mm was implemented for all tests, with indentation

rates ranging from 0.1 to 10 mm/s. A spherical steel indenter was implemented for these experiments and had a radius of curvature equal to 25.6 mm and a diameter of 20 mm. Temperature setpoints of 2°C, -10°C, and -20°C were utilized across tests. Wells et al. (2010) completed similar tests to those completed by Barrette et al. (2002). Wells et al. (2010) utilized a spherical steel indenter of similar radius of curvature and diameter of 25.6 mm and 20 mm, respectively. For these experiments the indentation depth was varied between 3 and 20 mm, with indentation rates from 0.2 to 10 mm/s being implemented across tests at a constant temperature of -10°C.

In order to more accurately investigate the indentation of rock particles into a confined ice specimen, the experiments outlined in this paper implement similar methods to those utilized in single steel indenter tests. The present experiments utilize similar principles to previously completed spherical steel indentation experiments, however these experiments implemented individual unconstrained rock particles which are compressed between two confined ice specimens mounted to the top and bottom plates of the MTS frame to ensure only ice and rock came into contact during the experiments. The experiments outlined in this paper primarily investigated the effects of changes in indentation rate as well as the relative spacing from previously formed damage zones on observed pressures and forces. Based on observed similarities between the underlying principles and observed effects in these tests completed using unconstrained rock particles, a comparison has been conducted between the results of the experiments outlined in this paper and those observed in previously completed spherical steel indentation experiments. Both the results of the particle indentation experiments and the comparison with spherical steel indentation tests are outlined below.

This paper utilizes methods similar to those implemented for single steel indenter tests to investigate the indentation of rock particles into a confined ice specimen. The main difference in the present experiments is that individual rock particles are compressed between two confined ice specimens mounted to the top and bottom plates of the MTS frame to ensure only ice and rock came into contact during these experiments. In these tests, the effects of changes in indentation rate and the relative spacing from previously formed damage zones on resulting force and pressure trends were investigated.

EXPERIMENTAL SETUP AND DESIGN

All tests throughout this experimental program were completed through the use of ice specimen with dimensions 11”x8”x2”, which were fabricated by crushing freshwater, polycrystalline ice into ice seeds, of grain size 4-10 mm. The ice seeds were frozen into ice specimen with chilled filtered tap water cool to near freezing in the cold room. The water was poured into the void space within a metal mold and allowed to freeze completely. To ensure the sample would freeze evenly, the ice seed was lightly compacted into an even layer as the water was poured to ensure a uniform surface and to remove any air bubbles within the specimen. In order to allow for the ice to freeze in layers, this process was repeated up to three times for a single specimen, where one layer was poured, flattened, and allowed to freeze in the cold room freezer at -10°C. Each layer would take up to 90 minutes to freeze completely, at which point the ice seed and cooled water would again be filled over the frozen layer, flattened, and allowed to freeze. Layers would be frozen until the entire sample mold was filled, at which point the sample was allowed to finish freezing completely for anywhere from 12-24 hours. This layered freeze method allows the ice block to freeze as one

cohesive block with minimal cracking, air bubble formation, and irregularities. Freezing was additionally conducted with a pane of insulating foam placed over the exposed top layer of the ice specimen to ensure directional freezing. This same process of crushing seed ice, flooding and freezing the ice was implemented for a single large layer to produce the bottom ice specimen.

A high-capacity MTS load frame was implemented for all testing in this experimental program. The test apparatus was located in the cold room facility at Memorial University's thermodynamics laboratory, as shown in Figure 1 below. Ice blocks were affixed to the MTS load frame and were loaded in order to simulate local compression and embedment of rock particles into the ice. The primary upper ice specimen was affixed to the upper mounting plate on the MTS crosshead and remained fixed in place during the test. The bottom-mounted ice specimen was fixed in the soil box, which was attached to the MTS base plate attached to the vertical hydraulic ram which experienced purely vertical displacement at a fixed indentation rate.

Figure 1. MTS load frame with ice specimen and soil box affixed.

To ensure full indentation for each test, a rock particle of known dimensions was placed on the bottom ice specimen (soil box) and was brought up to a position as close as possible with the ice specimen above, as can be seen in Figure 2 below. The top ice specimen position was adjusted such that indentation was conducted on pristine ice areas. Once the ice specimens no

longer had suitable areas of pristine ice to conduct the indentation tests, new ice specimens were prepared.

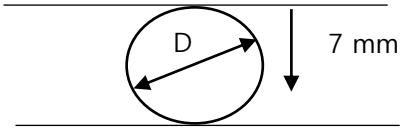

Figure 2. Schematic showing placement of rock particle prior to indentation.

The population of rock particles used in this experimental program were collected from a sieved population size between 3/8”–3/4”. Statistical analysis of these rocks was completed to determine the mean rock particle diameter, which was determined to be 13 mm. For the purpose of the work presented herein, the mean diameter value D was used to define the relative spacing for rock placement away from the damage zones at the indentation sites from prior tests and was also implemented to define bounds for the uniform distribution of rock sizes for modelling rock populations. For these single particle indentation tests the location of indentation was varied between tests, however this was found to have no significant effect on the results and is not considered in the present paper, full analysis of these effects can be found in previously published papers (Fitzpatrick et al., 2022). For all experiments, rock particles were indented to a depth of 7 mm beyond the initial point of contact between the particles and the top surface of the ice sample (Figure 2). The geometry of the rock particles was not directly characterized but were observed to be Coarse Aggregate/Crushed Stone with an overall irregular shaped and surface conditions that were observed to be jagged, smoothed edges and a rough surface texture. The MTS was outfitted with a load cell as well as a linear variable differential transformer (LVDT) displacement sensor which allowed for time series data to be collected. Photographs of the pristine ice, as well as damaged ice zones surrounding the particle-ice contact regions after indentation were taken.

RESULTS AND DISCUSSION

Experimental Results for Single Particle Indentation

Sixty-six (66) tests in total were completed throughout this experimental program, with repetitions of up to 10 tests per setpoint. These tests consisted of purely vertical indentation on single particles with no horizontal motion being imposed. The parameters of indentation rate and indentation site spacing were varied. As previously mentioned, the effects of indentation site spacing were found to have no effect on ice failure mechanics and are not considered in the analysis presented in this paper, full details of this can be found in previously completed papers (Fitzpatrick et al., 2022). For the purposes of this analysis, the representative case of 5D spacing will be used. Of these 66 total tests, 30 tests were completed with an indentation rate of 0.5 mm/s, an additional 30 tests were completed at an indentation rate of 10 mm/s, and finally, six tests were completed at an indentation rate of 0.01 mm/s.

The initial test cases of the experimental program without repetitions can be seen in the test matrix below in Table 1.

Table 1. Test Matrix.

Test No.	Test ID	v (mm/s)
1-10	2021_28_06_(1)-96-0.5	0.5
11-20	2021_28_06_(11)-65-0.5	0.5
21-30	2021_29_06_(1)-26-0.5	0.5
31-40	2021_06_07_(1)-96-10	10
41-50	2021_07_07_(1)-65-10	10
51-60	2021_08_07_(1)-26-10	10
61	2021_13_07_(1)-96-0.01	0.01
62	2021_13_07_(2)-65-0.01	0.01
63	2021_13_07_(3)-26-0.01	0.01

In the above testing matrix, v represents indentation rate in mm/s. All tests were completed with medium sized rock, to a depth of 7 mm with a nominal set point temperature of -10°C.

Effects of Indentation Rate

In order to effectively investigate the effects of rate on particle indentation, testing was completed at three different indentation rates, 0.01 mm/s (slow), 0.5 mm/s (moderate) and 10 mm/s (fast). These indentation rates were selected based on similar spherical steel indenter tests within the literature (Barrette et al., 2002; Wells et al., 2010; Browne et al., 2013). Plots representing three separate tests completed at these three indentation rates for 5D spacing can be seen below in Figure 3. Trends observed from test completed at an indentation rate of 0.01 mm/s exhibit evidence of a combination of ductile and brittle failure, with two events which were determined to be repeated crushing events, as described by Wells et al. (2010), that can be observed near the end of indentation. This cyclical loading is typical in compressive ice failure for higher rates (Barrette et al., 2002); however, it presents in these slow tests as oscillation when plotted against indentation depth due to the very slow indentation rate. Additionally, it is noted that for these slow tests, similar tests completed from smooth indenter tests would typically present more creep-dominated behavior (Wells et al. 2010) with repeated crushing events occurring at higher rates (Barrette et al., 2002), however the localized spalling which was triggered under these conditions is likely contributed to irregularities in the ice-particle contact geometry arising from asperities on the natural rock particles. Observations from the test completed at a moderate rate of 0.5 mm/s show a continuous increase in load with a localized spall occurring near the beginning of indentation. This localized spalling is associated with slow crushing failure of the sample, and this corresponds with a failure mode which is typically referred to as a ‘ductile’ failure. ‘Ductile’ failure corresponds with a slow, continuous flow of crushed ice beneath the contact zone. Finally for tests completed at the fast rate 10 mm/s, observations of a steady increase in load are shown as the sample undergoes typical phases of dynamic loading, with larger spalls and associated load drops being observed near the end of indentation.

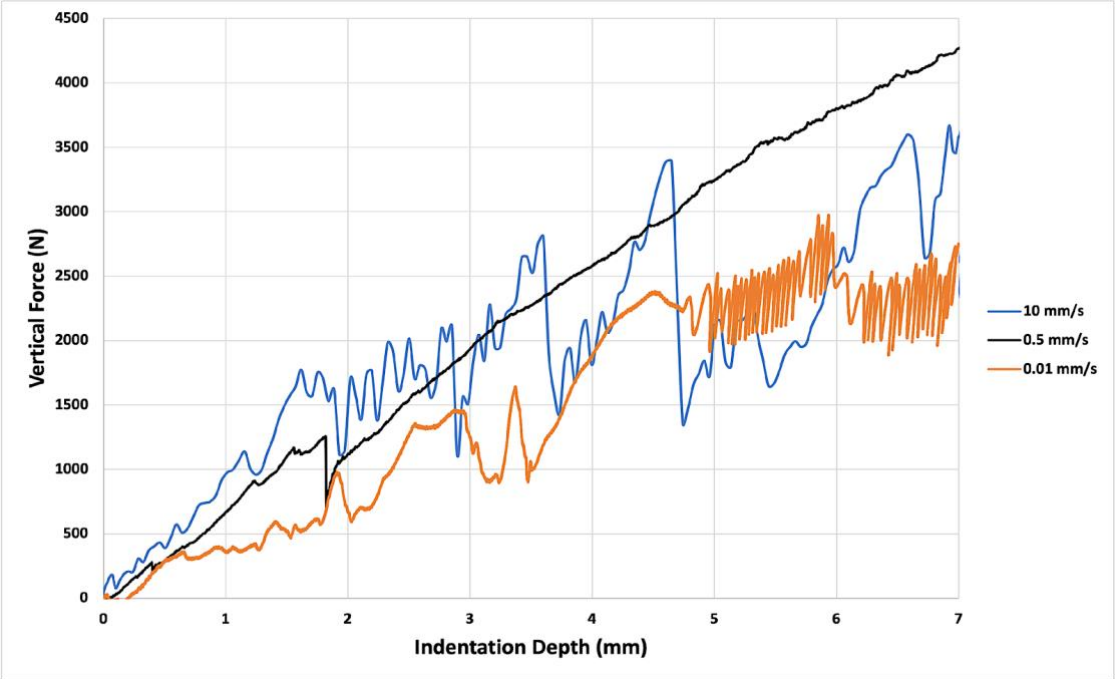

Figure 3. MTS load cell data for 3 tests: Slow speed (Orange); Moderate speed (Black); Fast speed (Blue) completed at 5D (65 mm) spacings.

The maximum observed forces and pressure were compiled for all separate tests completed at 0.01 mm/s, 0.5 mm/s, and 10 mm/s in order to investigate the effects of rate on peak force and pressure. The forces were taken directly from the force trace data obtained from the MTS, can be seen in Figure 4 (a) below, which shows an aggregate plot of tests completed at 0.01 mm/s, 0.5 mm/s, and 10 mm/s for a spacing case of 5D. The highest peak forces were observed for the moderate rate case of 0.5 mm/s, and the smallest were observed at slow rates of 0.01 mm/s. For fast rates of 10 mm/s the peak forces were moderately higher but remained lower overall. The peak pressures were calculated based on the nominal projected area of the rock particle assuming maximum indentation and can be seen in the aggregate pressure plot below, Figure 4(b). Peak pressures were observed to be largest for moderate rates of 0.5 mm/s, smallest at slow rates of 0.01 mm/s, and moderately higher at fast rates of 10 mm/s. This behavior is consistent with the trends observed for the force trace data.

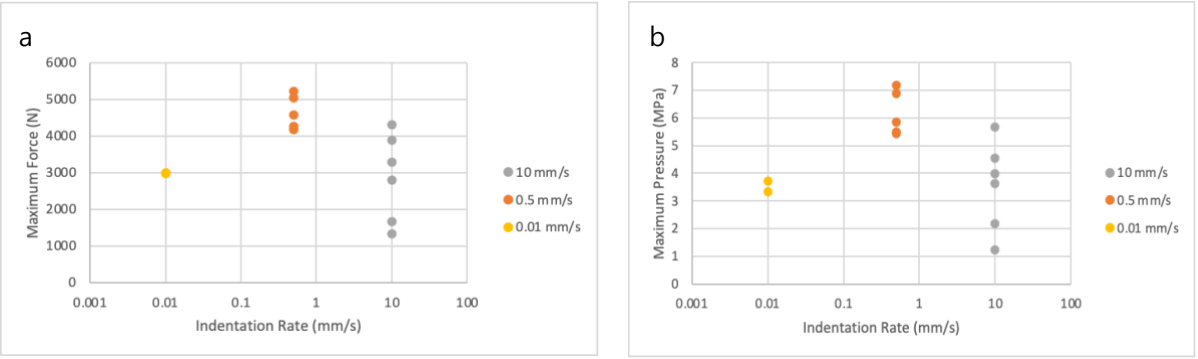

Figure 4. Aggregate maximum observed force (a) and pressure data (b), 5D spacing.

The behavior noted above is consistent with reported ice strain rate behavior from Wells et al. (2010) wherein slow rates result in ductile failure for which peak forces increase as rate increases, which then transition to mixed mode failure characterized by higher peak loads, and ultimately brittle failure at higher rates that exhibit lower peak forces.

Images of the damaged ice surface taken after indentation are shown in Figure 5 below. These images show damage patterns which indicate clear evidence of a mix of spalling and crushing occurring. The crushed and extruded ice, which can be observed in Figure 5 (c), exhibits characteristics which are consistent with ice formed due to localized pressure melting and refreezing. Additionally, it is noted that embedment and bonding of the ice particles in the upper ice specimen can be seen in Figure 5 (d). The ice failure processes observed below are very similar to the damaged zones which were observed during spherical steel indentation tests completed by Barrette et al. (2002), Wells et al. (2010), and Browne et al. (2013). These observed interaction mechanics between the ice and individual rock particles provide valuable insights that will serve to guide future experiments and modelling directions.

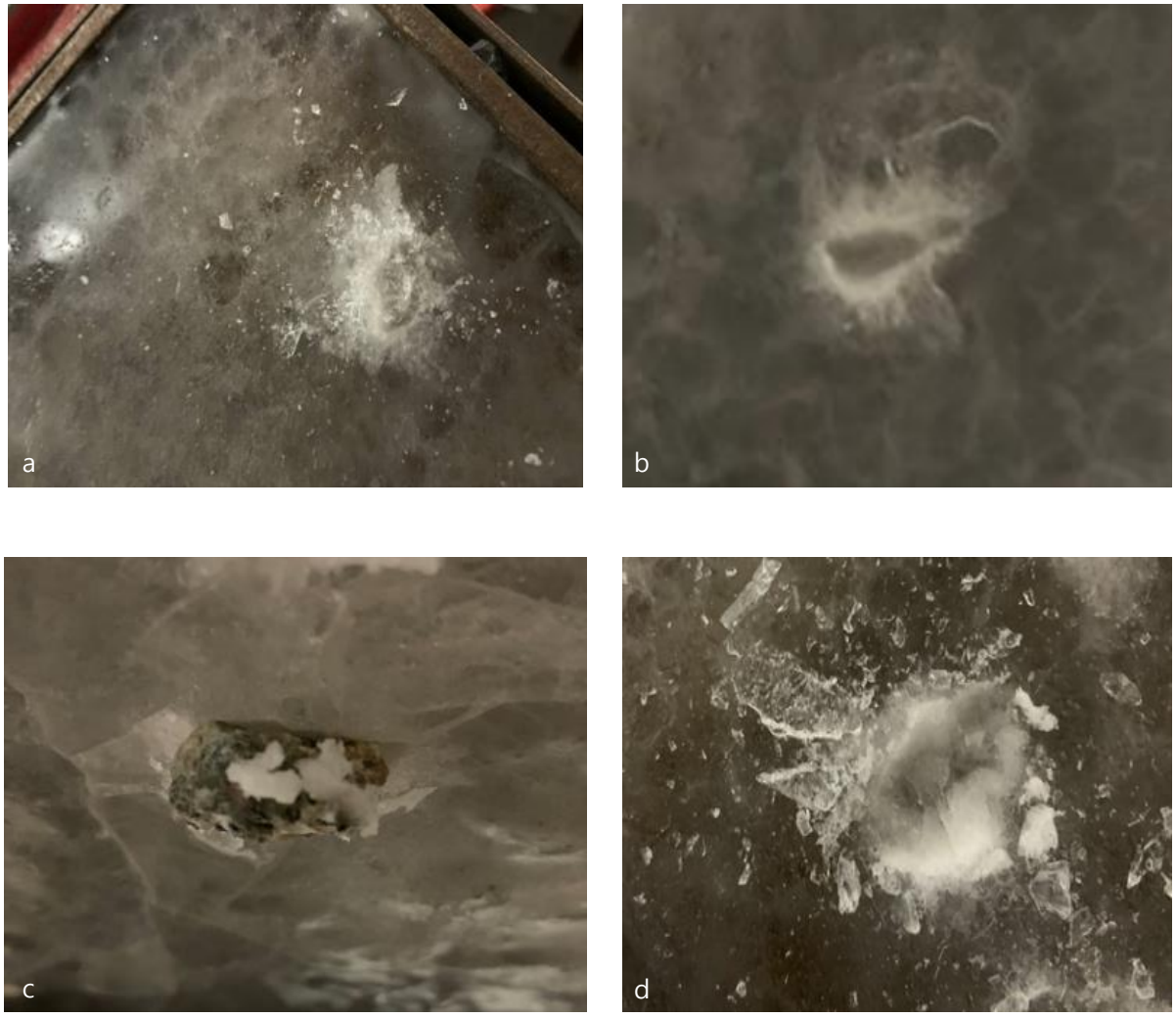

Figure 5. Images of bottom (left) and top (right) ice surfaces taken after testing for an indentation rate of 0.5 mm/s.

Comparison Between Single Particle and Spherical Steel Indentation Tests

Based on the analysis completed for single unconstrained rock particle indentation, particular interest was paid to the nature of indentation rate effects. The trends observed in the analysis of the indentation of single unconstrained rock particles was observed to be similar in nature to typical trends identified in research from spherical steel indentation tests. For the typical ranges of indentation rates implemented of 0.01 mm/s (slow rate), 0.5 mm/s (moderate rate), and 10 mm/s (fast rate) similar ice indentation research has been completed historically with spherical steel indenters of various geometries. Based on noted observed similarities between indentation of single unconstrained rock particles and these spherical steel indenter tests, a more direct comparison can be made in order to draw potential comparisons between the two testing scenarios. Research completed by Wells et al. (2010) presented Total Force versus Time graphs for indentation tests with a steel indenter of 20 mm in diameter for a range of indentation rates. Shown below in Figure 6 (a) and (b), are plots for indentation tests completed at 0.2 mm/s, and 10 mm/s. Similarities can be clearly seen between the force trace data patterns in these experiments completed by Wells et al. (2010) as those shown below in Figure 6 (c) and (d), which were observed for similar indentation rates of 0.5 mm/s and 10 mm/s tests using single unconstrained rock particles which were completed in this experimental research program.

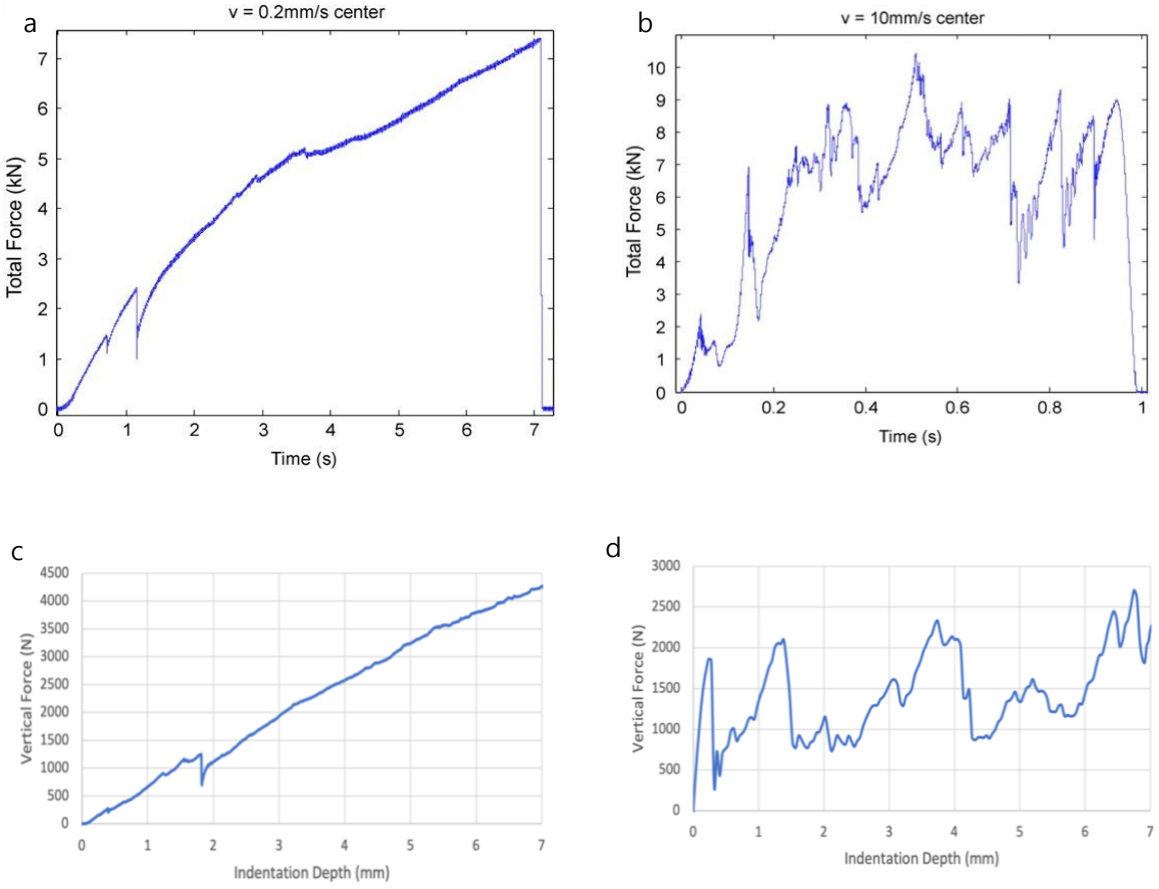

Figure 6. Plots from spherical steel indenter tests after Wells et al. (2010) at 0.2 mm/s (a) and 10 mm/s (b) and single unconstrained rock particle tests 0.5 mm/s (c) and 10 mm/s (d).

Direct comparison between the moderate rate test at 0.2 mm/s completed by Wells et al. (2010) shown in Figure 6(a) with tests completed in these experiments with unconstrained rock particles at the moderate rate test of 0.5 mm/s shown in Figure 6 (c), it can be seen that both plots exhibit typical phases of ductile failure, where the load continuously increases, with localized spalling occurring near the beginning of indentation as the sample experiences slow crushing failure; this corresponds with a failure mode which is typically referred to as a 'ductile' failure, and corresponds to a slow, continuous flow of crushed ice beneath the contact zone. Direct comparison between the fast rate test at 10 mm/s completed by Wells et al. (2010) show in Figure 6 (b) with tests completed in this paper with unconstrained rock particles at the fast rate test of 10 mm/s shown in Figure 6 (d), both plots can be seen to undergo typical phases of dynamic loading which is expected at this rate, where the load builds steadily and undergoes typical phases of dynamic loading, with larger spalls and associated load drops being observed near the end of indentation in both plots. Images taken after rock indentation shown above in Figure 5 (c, d) show clear evidence of a mix of spalling and crushing which is consistent with observed damaged zones formed during steel spherical indentation tests completed by Barrette et al. (2002) shown in Figure 7 (a), and by Wells et al. (2010) shown in Figure 7 (b).

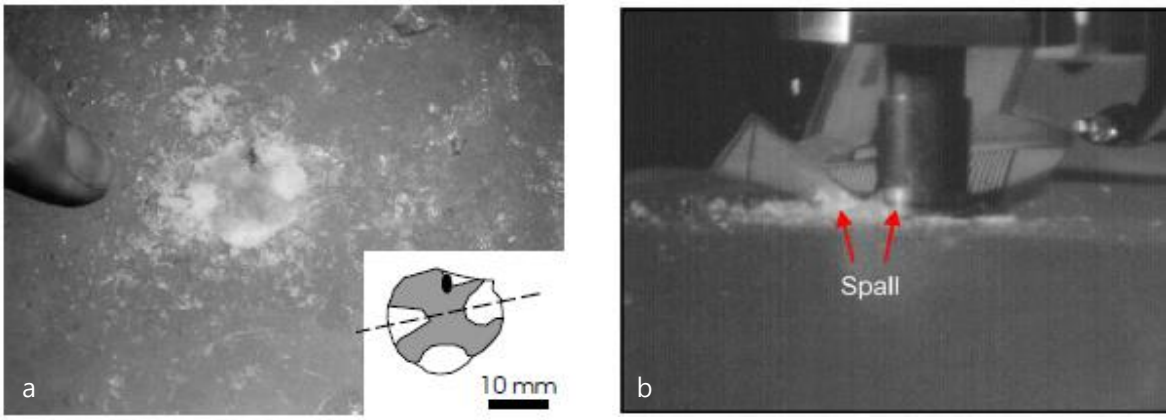

Figure 7. Images taken after testing for spherical steel indenter tests by (a) Barrette et al. (2002) and (b) Wells et al. (2010), show close agreement with results obtained for unconstrained rock particles shown in Figure 5 (c, d).

Images taken after indentation for a 0.2 mm/s test completed by Wells et al (2010), shown in Figure 7 (a), depicts a localized spall occurring as ice breaks away from the periphery of the damaged layer, leading to a sharp drop in load which corresponds to a decrease in contact area on the pressure sensor and the extrusion of material from under the indenter as seen Figure 7 (a). Wells et al. (2010) also notes the frequency and severity of localized spalling is observed to increase with increasing indentation rates, which is consistent with observations from single-particle rock indentation experiments completed at 0.5 mm/s during this experimental program and is substantiated by similar associated force and pressure trends. Clear similarities can be seen between the images taken after indentation from Wells et al (2010) in Figure 7 (a) and the experiments detailed in this paper shown in Figure 7 (c, d). Additional similarities are observed in indentation test done at a rate of 4 mm/s by Barrette et al (2002), Figure 7 (b). Barrette et al (2002) reports that fine-grained, pulverized ice was

produced due to indentation, with ice particles observed to range in size from a sub-mm, powder-like material to fragments up to 4 mm in maximum dimension. The indented ice surface had varying shape and surface area, surrounded areas defined by crushed ice with distinct radial cracks observed to be generated during the indentation event, which extended from the contact point to the edge of the mold. Barrette et al. (2002) observed recrystallized ice and microcracks well as the noted potential effects of pressure melting. Very similar spalling, crushing, recrystallization, and microcracking behavior is observed in the rock particle indentation tests which can be seen in Figure 7 (c, d) above.

CONCLUSIONS

In this paper, the effects of indentation rate of a single unconstrained rock particle under compressive ice loading were investigated alongside results from previously completed spherical steel indentation experiments. Force and pressure data collected during a series of single particle experiments taken at three indentation rates has been analyzed and compared with force and pressure data collected from previously completed series of experiments completed by Wells et al. (2010) and Barrette et al. (2002). From the analysis of single particle indentation tests, close agreement is observed between effects previously observed for indentation tests on ice with spherical steel indenters and those observed during ice-particle interactions. The observed differences between ice-rock and ice-steel indentation are believed to be caused primarily by local geometric variation in rock particle shape and has been observed to influence the dominant ice failure mechanisms and contribute to variability in measured forces and pressures. One of the most interesting observations, from an ice mechanics standpoint, was the observation that the rock particles tended to embed and adhere themselves into the ice under conditions that generated the highest loads ($v = 0.5$ mm/s). At these test conditions, the damaged ice immediately beneath the rock indentation site exhibited characteristics that correspond closely with observations of crushed/extruded ice associated with localized pressure melting and refreezing which was also observed during steel indentation tests. Overall, valuable insights into the underpinning mechanics were obtained and these outcomes suggest that these mechanisms may be important to the embedment and bonding of rock in ice during ice interactions with gravelly soils. Further testing under different temperature conditions, a more comprehensive range of indentation rates, and for different rock particle geometries is recommended.

ACKNOWLEDGEMENTS

The authors would like to thank the following people: Mr. Craig Mitchell, Mr. Matt Curtis, and Mr. Pritom Chakraborty for their assistance during laboratory testing at Memorial University. The authors would also like to thank Memorial University for use of their cold room facilities and C-CORE for their guidance and support of this collaboration. Funding from the Natural Sciences and Engineering Council of Canada (NSERC) is gratefully acknowledged.

REFERENCES

Barrette, P., Pond, J., and Jordaan, I., 2002, "Ice Damage and Layer Formation in Small Scale Indentation Experiments," Ice in the Environment, *Proceedings of the 16th International Symposium on Ice, IAHR*, Dunedin, New Zealand, Dec. 2–6, pp. 246–253.

Browne, T., Taylor, R., Jordaan, I., and Gürtner, A., 2013, "Small-Scale ice Indentation Tests with Variable Structural Compliance," *Cold Reg. Sci. Technol.*, 88, pp. 2–9.

Fitzpatrick, T., Taylor, R. S., Thijssen, J (2022). Compressive Failure of Ice During Indentation of Rock Particles. Proceedings of the ASME *2022 41st International Conference on Ocean, Offshore and Arctic Engineering. Volume 6: Polar and Arctic Sciences and Technology*. Hamburg, Germany. V006T07A011.

ISO 19906, 2019, *Petroleum and Natural gas Industries—Arctic Offshore Structures, International Organization for Standardization*, Geneva, Switzerland.

Jordaan, I. J., 2001, "Mechanics of Ice-Structure Interaction," *Eng. Fract. Mech.*, 68(17–18), pp. 1923–1960.

Schulson, E. M., and Duval, P., 2009, *Creep and Fracture of Ice*, Cambridge University Press, Cambridge, UK, p. 416.

Taylor, R. S., and Richard, M., 2014, "Development of a Probabilistic ice Load Model Based on Empirical Descriptions of High Pressure Zone Attributes," *International Conference on Offshore Mechanics and Arctic Engineering*, San Francisco, CA, June 8–13.

Wells, J., Jordaan, I., Derradji-Aouat, A., and Taylor, R., 2010, "Small-Scale Laboratory Experiments on the Indentation Failure of Polycrystalline Ice in Compression: Main Results and Pressure Distribution," *Cold Reg. Sci. Technol.*, 65(3), pp. 314–325.